Virologica Sinica (2021) 36:1154–1164
https://doi.org/10.1007/s12250-021-00399-3

www.virosin.org
www.springer.com/12250

RESEARCH ARTICLE

PML Suppresses Influenza Virus Replication by Promoting FBXW7 Expression

Hai-Yan Yan[1,2] · Hui-Qiang Wang[1,2] · Ming Zhong[1,2] · Shuo Wu[1,2] · Lu Yang[1,2] · Ke Li[3] · Yu-Huan Li[1,2]

Received: 16 December 2020 / Accepted: 29 March 2021 / Published online: 27 May 2021

Abstract

Influenza A viruses (IAV) are responsible for seasonal flu epidemics, which can lead to high morbidity and mortality each year. Like other viruses, influenza virus can hijack host cellular machinery for its replication. Host cells have evolved diverse cellular defense to resist the invasion of viruses. As the main components of promyelocytic leukemia protein nuclear bodies (PML-NBs), PML can inhibit the replication of many medically important viruses including IAV. However, the mechanism of PML against IAV is unclear. In the present study, we found PML was induced in response to IAV infection and ectopic expression of PML could inhibit IAV replication, whereas knockdown of endogenous PML expression could enhance IAV replication. Further studies showed that PML increased the expression of FBXW7 by inhibiting its K48-linked ubiquitination and enhanced the interaction between FBXW7 and SHP2, which negatively regulated IAV replication during infection. Moreover, PML stabilized RIG-I to promote the production of type I IFN. Collectively, these data indicated that PML inhibited IAV replication by enhancing FBXW7 expression in the antiviral immunity against influenza virus and extended the mechanism of PML in antiviral immunity.

Keywords Influenza A virus (IAV) · Promyelocytic leukemia (PML) · FBXW7 · RIG-I

Introduction

Influenza is an acute respiratory infectious disease caused by infection with influenza virus. Annual seasonal influenza epidemics and occasional emerging pandemics, such as 2009 swine influenza and sporadic emerging highly pathogenic avian influenza viruses (H5N1 and H7N9), became a serious health burden. Influenza A virus (IAV) belongs to *Orthomyxoviridae* family, which is a single-stranded, negative-sense RNA enveloped virus consisting of eight segmented genomes (Shaw and Stertz 2018). As an obligate pathogen encoding limited proteins, the influenza virus relies on host proteins and machinery to harbor infection and complete its life cycle (Krammer and Palese 2015).

Promyelocytic leukemia protein (PML), also known as MYL/RNF71/PP8675/TRIM19, is the organizer of the PML nucleus bodies (PML-NBs), which are dynamic cellular structures that contain many transiently and permanently localized proteins (Scherer and Stamminger 2016). On the basis of the splicing of a single gene, PML is divided into seven isoforms, PML I–VII (Nisole *et al.* 2013). All PML isoforms share the N-terminal region, which encodes the RBCC motif, while their C-terminal regions show remarkable variability and account for isoform-specific roles. In normal cells, PML proteins are distributed in discontinuous speckled patterns within the nucleus, known as components of the PML-NBs or PML

Supplementary Information The online version contains supplementary material available at https://doi.org/10.1007/s12250-021-00399-3.

✉ Yu-Huan Li
yuhuanlibj@126.com

✉ Ke Li
like1986@163.com

1 CAMS Key Laboratory of Antiviral Drug Research, Institute of Medicinal Biotechnology, Chinese Academy of Medical Sciences and Peking Union Medical College, Beijing 100050, China

2 Beijing Key Laboratory of Antimicrobial Agents, Institute of Medicinal Biotechnology, Chinese Academy of Medical Sciences and Peking Union Medical College, Beijing 100050, China

3 NHC Key Laboratory of Biotechnology of Antibiotics, Institute of Medicinal Biotechnology, Chinese Academy of Medical Science, Beijing 100050, China

oncogenic domains (PODs) subnuclear region (Negorev and Maul 2001). A few PML proteins, such as PML VIb and PML VIIb, are localized to the cytoplasm due to lack of the nuclear localization signal (NLS). PML, as the major component of PML-NBs, plays important roles in programmed cell death (Hsu and Kao 2018), cell senescence (Li *et al.* 2017), transcriptional regulation (Wang *et al.* 2018), genome stability (Chang *et al.* 2018), and antiviral defense (Blondel *et al.* 2010; Li *et al.* 2009; Alandijany *et al.* 2018; Chen *et al.* 2018; Chelbi-Alix *et al.* 2006; El Asmi *et al.* 2014).

PML has been demonstrated to display antiviral activities against DNA and RNA viruses *in vitro*, including vesicular stomatitis virus (VSV) (El Asmi *et al.* 2014), influenza virus (Li *et al.* 2009), herpes simplex virus (HSV) (Alandijany *et al.* 2018), human enterovirus 71 (EV71) (Chen *et al.* 2018) and rabies virus (Chelbi-Alix *et al.* 2006). Moreover, PML knockout mice were more sensitive to lymphocytic choriomeningitis virus (LCMV) (Kentsis *et al.* 2001) and VSV (El Asmi *et al.* 2014), which suggested that PML also had antiviral activity *in vivo*. It is well known that the replication of virus depends on a variety of host proteins in the nucleus. As an important subnuclear structure, PML-NBs are involved in the innate immune response of cells against viral invasion or the cellular antiviral response mediated by IFN. The relevant proteins PML, Sp100, PA28 and ISG20 were directedly induced by IFN and PML depletion reduced the ability of IFNs to resist viral infection (Chelbi-Alix *et al.* 1995), suggesting that PML-NBs could play an important role in IFN response. Although the function of PML NBs is not fully understood, some results show that they are increasingly recognized to be preferential targets for viral infections. Studies have shown that PML could play an important role in the antiviral action of IFNs via a higher activation of IRF3 (El Asmi *et al.* 2014), however, viruses have evolved a dual role against IFN-induced antiviral action. Viruses resist the antiviral activity by regulating PML expression and/or localization on nuclear bodies (Maul *et al.* 1993) and by inhibiting IFN signaling way (Everett and Chelbi-Alix 2007). Although the inhibitory activity of PML against DNA and RNA viruses has been partially elucidated, the mechanism of PML against influenza virus is still unclear.

FBXW7 (also known as FBW7/SEMO/hAgo/hCDC4) is one of the components of the Skp1-Cul1-F-box (SCF) ubiquitin-ligase SCF^{FBXW7}. SCF^{FBXW7} acts as a node for proteasomal degradation and plays an important role in cell proliferation and differentiation, lipid metabolism, and the maintenance of stem cell homeostasis (Welcker and Clurman 2008), including KLF2 (Wang *et al.* 2013), cyclin E2 (Moberg *et al.* 2001), c-Myc (Yada *et al.* 2004), Mcl-1 (Inuzuka *et al.* 2011) and Notch (Tsunematsu *et al.* 2004). FBXW7-deficient mice are more sensitive to RSV, VSV and influenza A virus infection and decreases type I interferon production. In addition, Song *et al.* showed that FBXW7 degraded the phosphorylated Src homology-2 domain-containing phosphatase 2 (SHP2), which negatively regulated the RIG-I/IRF3 signaling pathway and innate antiviral immunity (Song *et al.* 2017). However, the relationship between PML and FBXW7 during influenza virus infection has not been reported.

In this study, we confirmed the effect of PML against influenza virus and mainly explored the anti-influenza virus mechanism of PML for the first time. It provides a new idea for the discovery of anti-influenza virus targets and a theoretical basis for revealing the function of PML.

Materials and Methods

Cells and Viruses

Madin-Darby canine kidney (MDCK) cells, human lung adenocarcinoma epithelial cells (A549) and human embryonic kidney 293 T/17 cells (HEK293T/17) were obtained from American Type Culture Collection (ATCC); RAW264.7 cells were purchased from Cell Bank of the Chinese Academy of Sciences (Shanghai, China). MDCK cells were grown in minimum essential medium (MEM) supplemented with 10% fetal bovine serum (FBS), antibiotics (100 U/mL penicillin and 100 μg/mL streptomycin), and 1% MEM nonessential amino acid solution. A549 cells were cultured in F12K medium supplemented with 10% FBS and antibiotics. Human embryonic kidney 293 T/17 (HEK293T/17), and RAW264.7 cells were cultured in Dulbecco's modified Eagle's medium (DMEM) supplemented with 10% FBS and antibiotics.

Influenza virus A/Fort Monmouth/1/1947 (FM1, H1N1) was purchased from the ATCC (VR-97), A/HanFang/359/95 (HanFang, H3N2) strain was kindly provided by Professor Yuelong Shu at the Institute for Viral Disease Control and Prevention, China Centers for Disease Control and Prevention, Beijing, China. Viral stocks were prepared by propagating them in 10-day-old embryonated Chicken eggs for 48 h.

Compounds, Plasmids, and Antibodies

Bafilomycin A1 (Baf A1) was purchased from Sangon Biotech (Shanghai, China). Cycloheximide (CHX) was purchased from MedChemExpress (NJ, USA). MG132 was obtained from Selleckchem (TX, USA).

The plasmids of pcDNA3.1-Myc-PMLIV, pcDNA3.1-Flag-Ub, and pcDNA3.1-Myc-FBXW7 were provided by Professor Zhuowei Hu from the institute of Materia

Medica, Chinese Academy of Medical Sciences and Peking Union Medical College (Beijing, China). pCMV3-FBXW7-His was purchased from Sinobiological Inc (Beijing, China). A cDNA encoding the full-length human SHP2 were cloned into the pcDNA3.1(+) vector. All constructs were confirmed by sequencing. PML-siRNA (si-PML) and Control-siRNA (si-NC) were purchased from Santa Cruz (sc-36284, CA, USA).

Antibodies against influenza A M2 (sc-32238) and influenza A NS1 (sc-130568) were obtained from Santa Cruz (CA, USA). The antibody against PML (NB100-59,787) was from Novus Biologicals (Colorado, USA). The antibody against FBXW7 (H5081-3D-1) was purchased from Abnova (Taipei, Taiwan). Antibodies against SHP2 (#3397), RIG-I (#3743), HA-Tag (#2367), Myc-Tag (#2276), β-Actin (#3700), Tubulin (#2148), Alexa Fluor 488-conjugated goat anti-mouse (#4408) or rabbit (#4412) IgG, and Alexa Fluor 647-conjugated goat anti-mouse (#4410) or rabbit (#4414) IgG were purchased from CST (Cell Signaling Technologies, USA). Antibodies against Histone H3 (17,168-1-AP), His-Tag (66,005-1-Ig), and Flag-Tag (66,008-2-Ig) were obtained from the Proteintech Group (IL, USA). HRP-conjugated secondary antibodies against mouse (HS201-01) or rabbit (HS101-01) IgG were purchased from TransGen (Beijing, China).

IAV Infection and Virus Titer Determination

A549 cells in a 6-well plate were transfected with the indicated plasmids. The cells were infected with IAV at a multiplicity of infection (MOI) of 0.2 at 24 h post-transfection. At 24 h post infection, cells were frozen and melted thrice, and the supernatant was harvested after centrifugation for removing cell debris. The virus titers were performed by measuring $TCID_{50}$. Confluent monolayers of MDCK cells were infected through tenfold serially diluted supernatant in 96-well plates. The medium was changed 2 h after virus infection. The cytopathic effect (CPE) of cells was observed at 48 h, and $TCID_{50}$ was calculated by Reed & Muench method.

Western Blot

Protein extracts (10 μg) were subjected to electrophoresis with 10% polyacrylamide gel and were blotted onto PVDF membranes (Millipore Corp.). The membrane was incubated with primary antibody overnight at 4 °C, followed by incubation with HRP-conjugated rabbit anti-mouse or goat anti-rabbit IgG. The signal was detected with an ECL kit.

Immunoprecipitation

HEK293T/17 cells were transfected with the indicated plasmids for 48 h. Cells were collected and lysed in M-PER mammalian protein extraction reagent that contained halt protease inhibitor cocktail (MA, USA) for 30 min at 4 °C and then centrifuged at 12,000 $\times g$ for 20 min. The supernatants were incubated with 4 μg of the indicated antibody overnight. Agarose beads were added to the lysate for 3 h and then washed with washing buffer. The samples were boiled for 5 min and analyzed by SDS-PAGE and immunoblotting.

Quantitative Real-time PCR (qRT-PCR)

For intracellular viral RNA quantification, the total RNA was extracted from the cells by using RNeasy Mini Kit (Qiagen) according to the manufacturer's instruction. Then, quantitative reverse transcription PCR (qRT-PCR) was performed using the TransScriptII Green One-Step qRT-PCR SuperMix Kit (TransGen Biotech Co., Ltd. Beijing, China) according to the protocol. The sequences of the primers are depicted in Supplementary Table S1.

Indirect Immunofluorescence Assay

A549 cells were grown in coverslips in 12-well plates overnight. Cells were incubated for 2 h with the influenza virus at 37 °C in 5% CO_2 for adsorption. After 2 h, inoculum was decanted, and infected cells were supplemented with maintenance medium. After 18 h, A549 cells were washed three times with PBS and then fixed for 10 min with 4% paraformaldehyde. The cells were permeabilized in 0.5% Triton X-100 for 15 min. The slides were then blocked with 3% BSA for 1 h at room temperature and further incubated with the influenza virus M2 antibody overnight at 4 °C. After washing three times with 0.1% TBS-Tween, cells were incubated with Alexa Fluor 488 anti-mouse IgG for 1 h. The nucleus was stained with DAPI (Beyotime, Shanghai). Photos were taken with an Olympus TH4-200 microscope.

For colocalization studies with FBXW7-His and PML, fixed A549 cells were permeabilized in 0.5% Triton X-100 for 15 min and blocked with 3% BSA for 1 h at room temperature. The cells were incubated with rabbit anti-His-tag and mouse anti-PML antibody overnight at 4 °C, rinsed with TBST, and stained with Alexa Fluor 647 anti-rabbit IgG and Alex Fluor 488 anti-mouse IgG for 1 h. The slides were mounted with DAPI. Images were acquired with a Zeiss LSM 710 microscope.

Statistical Analysis

All data were analyzed by the SPSS 19.0 software, comparing with groups using one-way ANOVA, and the two independent groups were analyzed via Student's *t*-test. Data are showed as means ± SD. Statistical differences were considered significant at $^{*}P < 0.05$ and $^{**}P < 0.01$.

Results

IAV Infection Upregulates the Expression of PML in A549 Cells

To determine whether IAV infection impacted PML expression, A549 cells were infected with at various multiplicity of IAV (MOI = 2, 0.2, 0.02, and 0.002), and the protein and mRNA levels were determined by Western blot and qRT-PCR. As shown in Fig. 1A and 1B, both the protein and mRNA levels of PML were upregulated after IAV infection. Moreover, the protein and mRNA levels of PML were significantly upregulated at 8 h post-infection (pi) and 24 h pi (Fig. 1C and 1D). The results suggest that the expression of PML was significantly induced by IAV infection in a time- and dose-dependent manner. Previous studies had shown that the PML-NBs changed differently under different cell types, cell cycles, or external stimulations (Batty *et al.* 2012). To determine whether IAV infection altered PML nuclear bodies, we performed immunofluorescent staining experiment. As shown in Fig. 1E, the number of PML nuclear bodies (PML-NBs) increased in IAV-infected cells compared with uninfected cells at 24 h pi. These data indicate that IAV infection upregulates the expression of PML and increases the number of PML-NBs in A549 cells.

PML Inhibits IAV Infection

To evaluate the effects of PML on IAV replication, A549 cells were transfected with Myc-PML plasmid and then infected with IAV. As shown in Fig. 2A, 2B and 2C, compared to the control cells, IAV NS1 and M2 protein level (Fig. 2A and 2C) and RNA level (Fig. 2B) significantly decreased. In addition, we observed that the viral titers dose-dependently decreased in the cells transfected with external PML (Fig. 2D). In addition, with the expression of external Myc-PML in the A549 cells, IAV replication significantly decreased. To investigate whether reducing the expression of PML can enhance IAV replication, A549 cells were transfected with si-PML or si-NC.

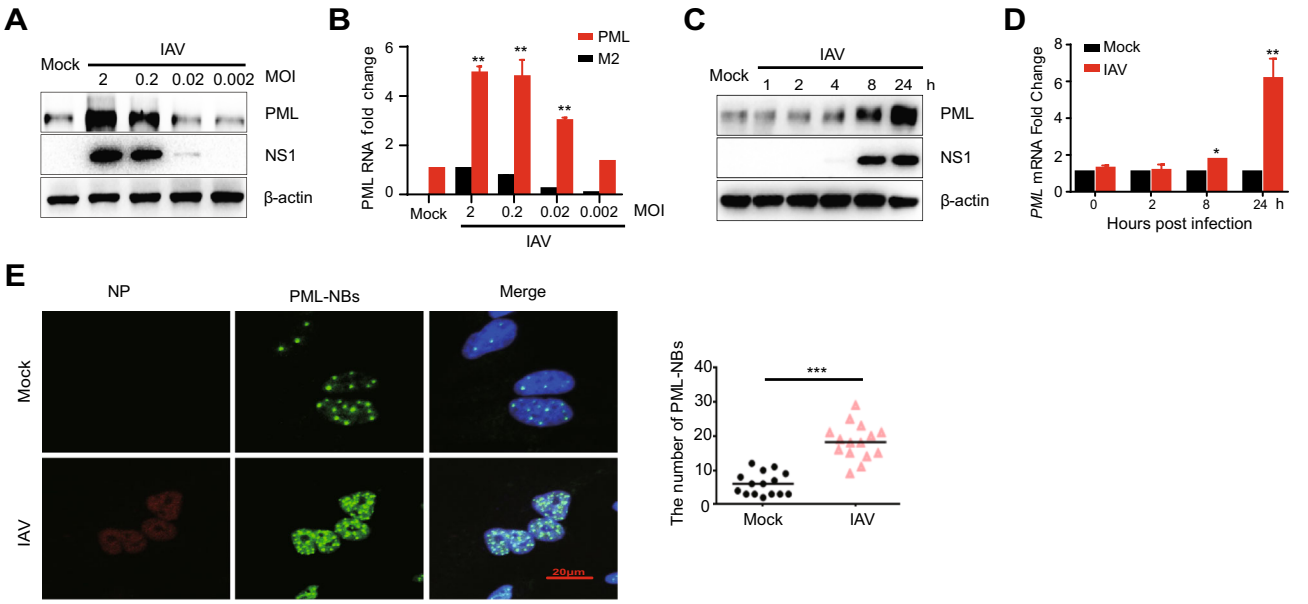

Fig. 1 IAV infection upregulates PML expression in A549 cells. A549 cells were infected with IAV (H1N1/FM1, MOI = 2, 0.2, 0.02, 0.002) for 2 h. **A** After 24 hpi, the protein levels of IAV NS1 and PML were analyzed by Western blot(Without special instructions, the strain of H1N1/FM1was used in all experiments.). **B** RNA from cells was extracted at 12 hpi and was subjected to qRT-PCR analysis to determine the expression of PML and M2. **C** A549 cells were infected with IAV (MOI = 0.2). After 1, 2, 4, 8, and 24 h, the protein levels of IAV NS1 and PML were analyzed by Western blot. **D** PML mRNA was examined by qRT-PCR at 0, 2, 8, and 24 hpi. The experiments were performed in triplicate. Each value represents means ± SD. $^{*}P < 0.05$; $^{**}P < 0.01$ versus 0 h group. **E** A549 cells were infected with IAV, and fixed at 24 hpi (MOI = 0.2) and subjected to immunofluorescence to detect NP (red) and PML nuclear bodies (PML-NBs, green). Nuclei stained by DAPI are shown in blue. Scale bar is 20 μm. The number of PML-NBs was counted in a single cell (n = 15).

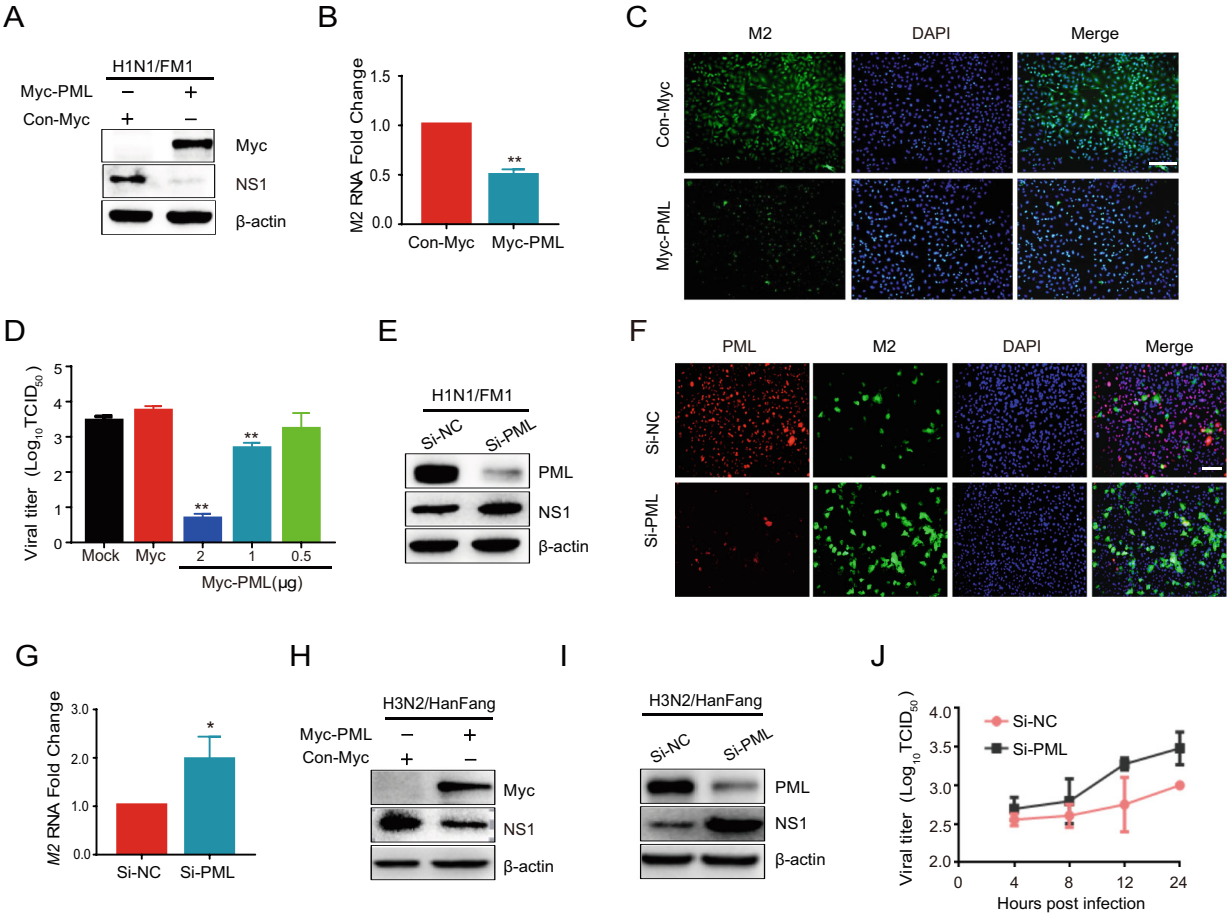

Fig. 2 PML inhibits IAV replication in A549 cells. A549 cells transfected with Myc-PML plasmid (1 μg) or Myc vector (1 μg) using lipofectamine 3000 reagent for 24 h. Then, the cells were infected with IAV (MOI = 0.2) for 2 h. **A** After 24 hpi, PML and IAV NS1 protein expression was analyzed by Western blot. **B** The total RNA was extracted at 8 hpi (MOI = 0.2) and then subjected to qRT-PCR to analyze the IAV M2 RNA level. **C** A549 cells were fixed at 24 hpi and then subjected to immunofluorescence to detect IAV M2 (green). Nuclei stained by DAPI are shown in blue. Scale bar is 100 μm. **D** After transfection with Myc-PML plasmid (2, 1, 0.5 μg) or Myc vector (1 μg) for 24 h, A549 cells were infected with IAV for 2 h, and frozen and melted thrice at 24 hpi. Virus from the supernatant was harvested and viral titers were quantified by measures for $TCID_{50}$. Results were presented as $\log_{10}$ values of the mean viral load ± SD. **E–G** A549 cells were infected with IAV (MOI = 0.2) for 2 h after transfection of si-PML (20 nmol/L) and si-NC (20 nmol/L) for 24 h. After 24 hpi, PML and IAV NS1 protein expression were analyzed by western blot and immunofluorescence (**E** and **F**). The cellular RNA was extracted at 8 hpi (MOI = 0.2) and then subjected to qRT-PCR to analyze the IAV M2 RNA level (**G**). **H-I** A549 cells transfected with Myc-PML plasmid (1 μg) and Myc vector (1 μg) or si-PML (20 nmol/L) and si-NC (20 nmol/L) for 24 h were infected with IAV (H3N2/HanFang, MOI = 0.2) for 2 h. PML and IAV NS1 protein expression was analyzed by Western blot at 24 hpi. **J** After transfection with si-PML (20 nmol/L) and si-NC (20 nmol/L) for 24 h, A549 cells were infected with influenza virus at MOI of 2. Virus titer was determined by CPE assay with MDCK cells. Results were expressed as $\log_{10}$ values of the mean viral load ± SD. The experiments were performed in triplicate, $^{*}P < 0.05$; $^{**}P < 0.01$ versus con group.

Indeed, knockdown of PML enhanced the protein and mRNA levels of IAV (Fig. 2E–2G). For the influenza A virus H3N2 subtype, overexpression of PML in A549 cells inhibited the replication of influenza virus, and knockdown of PML showed higher susceptibility to influenza virus (Fig. 2H and 2I). We further confirmed that virus titer was significantly increased in the PML knockdown A549 cells compared with those in the Si-NC group (Fig. 2J). Taken together, these data indicate that PML inhibits IAV replication.

PML Interacts with FBXW7

As a host limiting factor, PML exhibits antiviral activity against DNA viruses and RNA viruses through a variety of mechanisms. Our results shows that PML has a positive inhibitory effect on IAV replication, which is consistent with previous report (Li e*t al.* 2009). Previous report had suggested that FBXW7, as an E3 ubiquitin ligase, played an important role in the natural immunity against VSV or influenza A virus (Song *et al.* 2017). Therefore, we speculate that PML may affect IAV replication by regulating

FBXW7. First, the interaction between PML and FBXW7 needs to be confirmed. Immunofluorescence imaging showed that the colocalization of PML and FBXW7 in A549 cells (Fig. 3A). Co-IP assay also showed that PML interacted with FBXW7 in PML and FBXW7 exogenous expressed HEK293T/17 cells (Fig. 3B). We also examined whether Myc-PML or His-FBXW7 could interact with endogenous PML or FBXW7 in the context of IAV-infected cells. The forward and inverse Co-IP results also confirmed that PML interacted with FBXW7 (Fig. 3C and 3D) in IAV-infected cells. Previous study reported that FBXW7 could translocate from nucleus into cytoplasm and stabilize RIG-I during virus infection, however, PML IV protein is mainly located in the nucleus. To confirm the location of interaction between PML and FBXW7, we utilized Co-IP assay to observe the interaction along with IAV infection in cytoplasm and nucleus separately. Interestingly, we found that PML both interacted with FBXW7 in cytoplasm and nuclear (Fig. 3E), which inspired us to identify the potential function of PML in FBXW7-triggered antiviral innate response.

PML Represses Ubiquitylation and Degradation of FBXW7

Since PML interacted with FBXW7 in cytoplasm, we suspected whether PML played an anti-IAV role by affecting the cytoplasmic FBXW7. Next, we assessed the effect of PML overexpression or knockdown on FBXW7. The effect of overexpression of PML on FBXW7 transcription was detected and there was no significant change in the mRNA level of FBXW7 after overexpression of PML (Fig. 4A). However, overexpression of PML increased the protein level of FBXW7, whereas knockdown of PML significantly inhibited FBXW7 protein expression compared with si-NC (Fig. 4B and 4C). Since PML did not affect FBXW7 transcription, but upregulated FBXW7 protein levels, this suggested that PML may regulate the degradation of FBXW7. Ubiquitination is an important form of posttranslational protein modification, which is involved in the regulation of protein function and maintenance of cell life activities. Therefore, we investigated whether PML regulated the ubiquitylation of FBXW7 protein. Overexpression of PML inhibited the ubiquitylation of FBXW7 and prolonged the half-life of

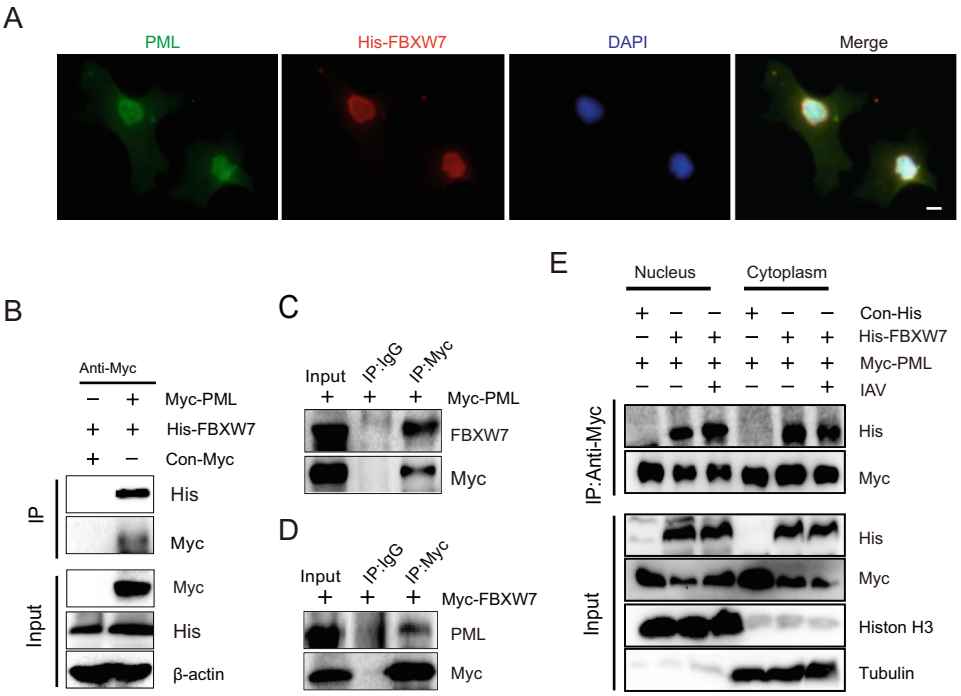

Fig. 3 PML interacts with FBXW7. **A** A549 cells transfected with His-FBXW7 for 24 h were infected with IAV (MOI = 0.2) for 2 h. After 36 hpi, A549 cells were fixed and subjected to immunofluorescence to detect PML (green) and His-Tag (red). Nuclei stained by DAPI were shown in blue. Scale bar is 20 μm. **B** HEK293T/17 cells were co-transfected with His-FBXW7 and Myc-PML plasmids for 36 h. The cell lysates were immunoprecipitated with anti-Myc beads and immunoblotted with anti-His antibody. **C** and **D** HEK293T/17 cells were transfected with Myc-PML and FBXW7 or Myc-FBXW7 and PML plasmids for 24 h. Coimmunoprecipitation and immunoblot analysis were conducted on HEK293T/17 cells infected with IAV at 24 hpi. **E** HEK293T/17 cells transfected with His-FBXW7 and Myc-PML for 24 h, then infected with IAV for 8 h. The cells are collected and then separated into nuclei and cytoplasm. The cell lysates were immunoprecipitated with anti-Myc beads in cytoplasm and nucleus separately.

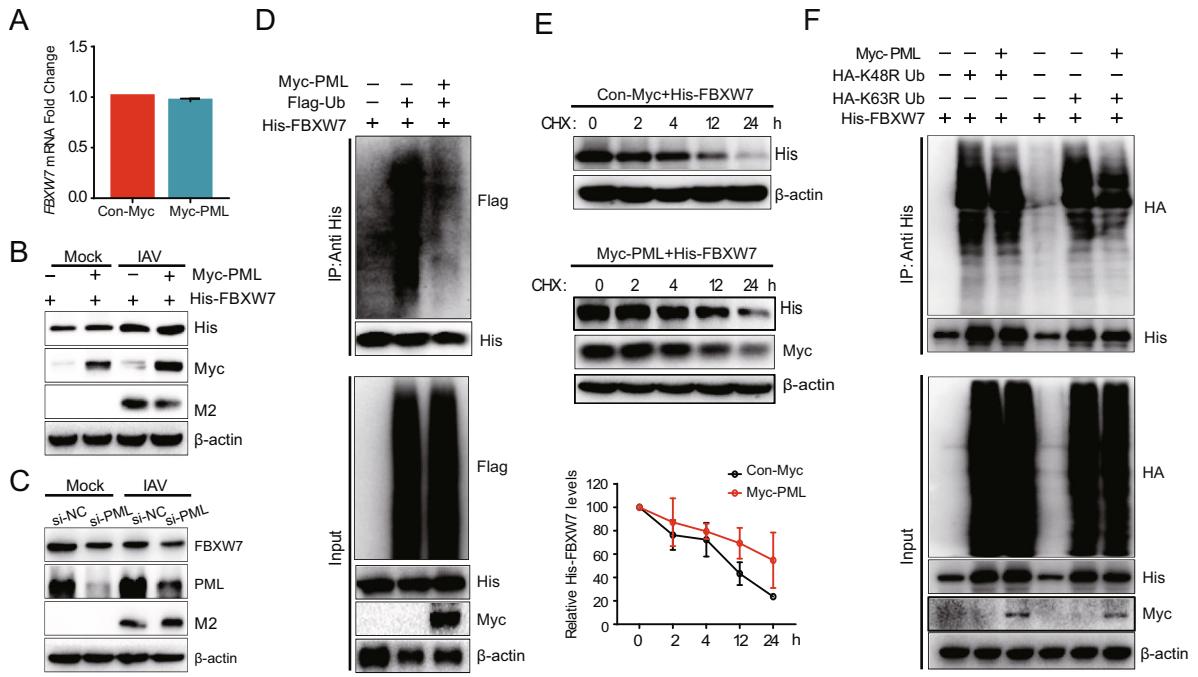

Fig. 4 Effects of PML on FBXW7 in A549 cells. **A** A549 cells transfected with Myc-PML plasmid (1 μg) or Myc vector (1 μg) for 24 h were infected with IAV (MOI = 0.2). The total RNA was extracted at 12 hpi (MOI = 0.2) and then subjected to qRT-PCR to analyze *FBXW7* mRNA level. **B** A549 cells co-transfected with Myc-PML plasmid (1 μg) and His-FBXW7 (1 μg) or with an empty vector were infected with IAV (MOI = 0.2) for 24 h. The expressions of His-FBXW7, Myc-PML, and IAV M2 protein were analyzed by western blot. **C** A549 cells transfected with si-PML (20 nmol/L) and si-NC (20 nmol/L) for 24 h were infected with IAV (MOI = 0.2) for 2 h. After 24 hpi, the PML, FBXW7, and IAV M2 protein expressions were determined by Western blot. **D** HEK293T/17 cells were co-transfected with His-FBXW7, Flag-Ub, and Myc-PML plasmids for 36 h with MG132 treatment for 6 h. The cell lysates were immunoprecipitated with anti-His beads and immunoblotted with anti-Flag antibody. **E** HEK293T/17 cells were transfected with His-FBXW7 and Myc-PML for 24 h and incubated with cycloheximide (CHX, 10 μg/mL) for indicated times. **F** HEK293T/17 cells were co-transfected with His-FBXW7, HA-K48R Ub, HA-K63R Ub, and Myc-PML plasmids for 36 h with MG132 treatment for 6 h. The cell lysates were immunoprecipitated with anti-His beads and immunoblotted with anti-HA antibody.

exogenous FBXW7 protein degradation (Fig. 4D and 4E). These results suggested that PML enhanced the protein level of FBXW7 by sustaining the stability of FBXW7. To determine which form of the polyubiquitin chains of FBXW7 was catalyzed by PML, we co-transfected HA-K48R Ub, HA-K63R Ub, Myc-PML, and His-FBXW7 plasmids into cells and then detected the polyubiquitination of FBXW7. Results showed that K48R-linked ubiquitination of FBXW7 did not change, but K63R-linked ubiquitination of FBXW7 decreased in overexpressing PML cells (Fig. 4F). These data indicated that PML mediated K48-linked ubiquitination of FBXW7.

PML/SHP2 Interaction Promotes the Degradation of SHP2

As reported previously, FBXW7 interacted with SHP2 and mediated the degradation and ubiquitination of SHP2, thus disrupting the SHP2/c-Cbl complex, which mediated RIG-I degradation and type I interferon signaling (Song *et al.* 2017). As PML had been shown to increase the FBXW7 protein expression, we suspected that PML may affect SHP2 and RIG-I and inhibit the IAV replication by promoting the production of type I IFN.

To determine whether PML interacted with SHP2, the Myc-PML and HA-SHP2 plasmid was transfected into HEK293T/17 cells. The total cell extracts were extracted and immunoprecipitated with anti-Myc or anti-HA antibody followed by Western blot analysis. The result showed that PML interacted with SHP2 (Fig. 5A and 5B). Further immunoprecipitation assay showed that PML interacted with endogenous SHP2 when HEK293T/17 cells were transfected with Myc-PML plasmids and infected with IAV for 24 h (Fig. 5C). Moreover, the level of SHP2 protein expression was decreased in A549 cells transfected with Myc-PML plasmid (Fig. 5D). The cycloheximide chase assay showed that overexpression of PML synergized with FBXW7 to decrease the half-life of intracellular SHP2 protein in HEK293T/17 cells (Fig. 5E). PML interacted with FBXW7 and SHP2, thereby forming an interaction complex between PML, FBXW7, and SHP2. To investigate the role of PML in the interaction between FBXW7 and SHP2, HEK293T/17 cells were co-transfected with Myc-PML and His-FBXW7 plasmids together and we

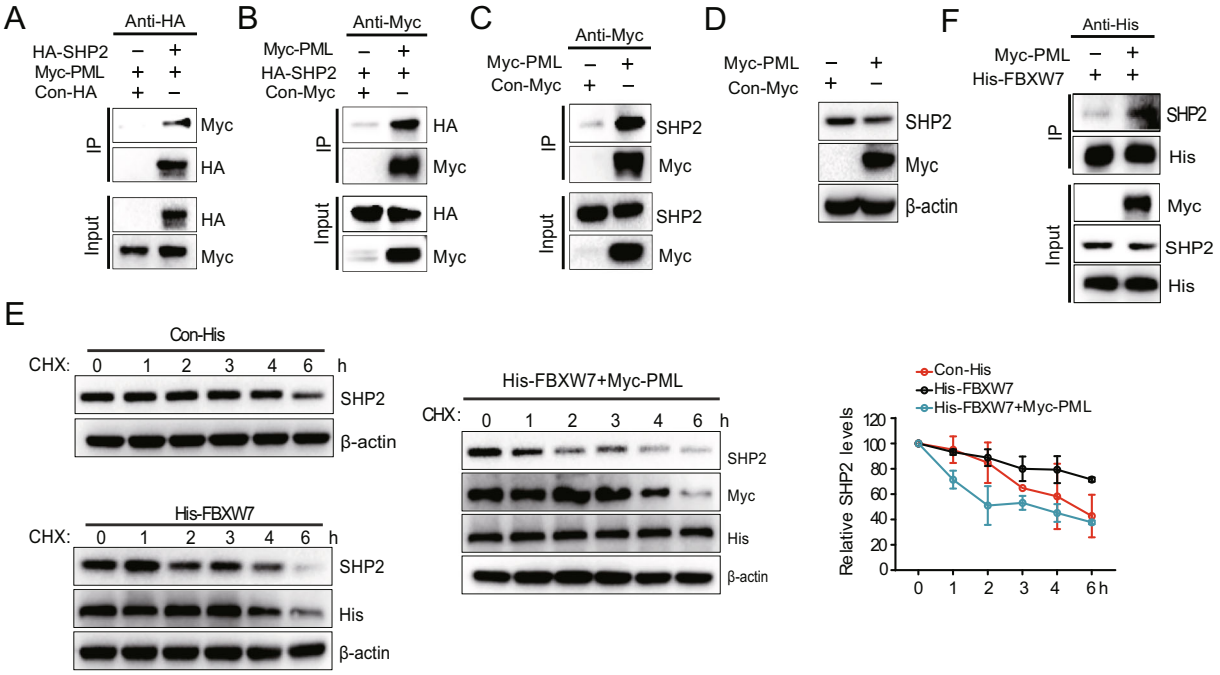

Fig. 5 PML enhances the interaction between FBXW7 and SHP2 and promotes degradation of SHP2. **A** and **B** HEK293T/17 cells were co-transfected with HA-SHP2 and Myc-PML plasmids for 36 h. The cell lysates were immunoprecipitated with anti-HA or anti-Myc beads and immunoblotted with anti-Myc or HA antibody. **C** HEK293T/17 cells were transfected with Myc-PML plasmids for 24 h. Coimmunoprecipitation and immunoblot analysis of HEK293T/17 cells infected with IAV at 24 hpi. **D** A549 cells were transfected with Myc-PML plasmid (1 μg) and Myc vector (1 μg) for 36 h. Myc-PML and SHP2 protein expression were analyzed by Western blot. **E** HEK293T/17 cells were transfected with Con-His, His-FBXW7, and Myc-PML for 24 h and incubated with cycloheximide (CHX, 10 μg/mL) for indicated times. The experiments were performed in triplicate. Each value represents mean ± SD. **F** HEK293T/17 cells were co-transfected with Myc-PML and His-FBXW7 for 24 h. The cell lysates were immunoprecipitated with anti-His beads and immunoblotted with SHP2 antibody.

observed that PML enhanced the interaction between FBXW7 and SHP2 (Fig. 5F). These data demonstrated that PML enhanced the interaction between FBXW7 and SHP2 and promoted degradation of SHP2.

PML Stabilizes RIG-I and Promotes the Production of Type I IFN

Considering the previous report that FBXW7 degraded SHP2 protein while SHP2/c-Cbl complex negatively regulated RIG-I, we speculated that PML may promote RIG-I protein expression (Song *et al.* 2017). To detect whether PML could affect the RIG-I, A549 cells were transfected with Myc-PML or si-PML with or without IAV infection. The results showed that the protein expression of RIG-I was significantly increased in both infected and non-infected cells with PML overexpression (Fig. 6A), while RIG-I was downregulated in PML knockdown cells (Fig. 6B). The cycloheximide chase assay showed that PML overexpression extended the half-life of endogenous RIG-I protein (Fig. 6C). These data indicate that PML regulates type I IFN signaling by protecting RIG-I from degradation. To further confirm the role of PML, we detected IFN-α and IFN-β mRNA levels in RAW264.7 cells that were transfected with Myc-PML and infected with IAV. PML overexpression cells displayed higher IFN-α and IFN-β mRNA level compared with control cells (Fig. 6D and 6E). Overall, these data demonstrated that PML stabilized RIG-I and promoted the production of type I IFN.

Discussion

In this study, the results showed that the protein and mRNA levels of PML and the number of PML nuclear bodies significantly increased after infection with influenza virus, indicating that PML protein was positively correlated with influenza virus infection. Reports indicated that overexpression of PML significantly delayed influenza viral replication rate in Caco-2 cells, and downregulation of PML expression by RNAi enhanced viral replication (Li *et al.* 2009; Chelbi-Alix *et al.* 1998). We also found that overexpression of PML IV in A549 cells inhibited the replication of subtype A/H1N1 (Fig. 2A–2D) and subtype A/H3N2 (Fig. 2G) viruses, and knockdown PML increased

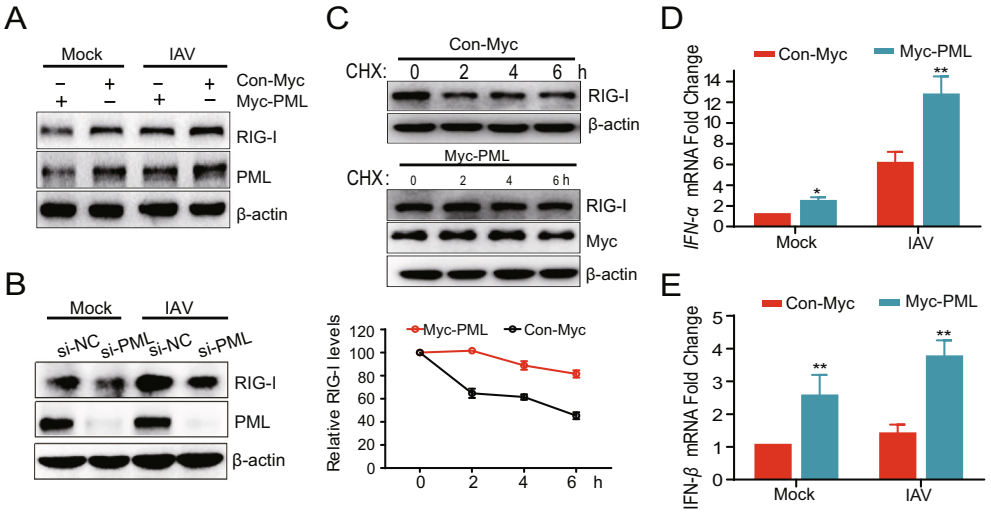

Fig. 6 PML represses the degradation of RIG-I and promotes type I IFN production. **A** A549 cells transfected with Myc-PML plasmid (1 μg) and Myc vector (1 μg) for 24 h were infected with IAV (MOI = 0.2) for 2 h. After 24 hpi, PML and RIG-I expressions were analyzed by Western blot. **B** A549 cells transfected with si-PML (20 nmol/L) and si-NC (20 nmol/L) for 24 h were infected with IAV (MOI = 0.2) for 2 h. After 24 hpi, PML and RIG-I expression were analyzed by Western blot. **C** A549 cells were transfected with Myc-Con or Myc-PML for 24 h and incubated with cycloheximide (CHX, 15 μg/mL) for indicated times. **D** and **E** RAW264.7 cells transfected with PML plasmid (1 μg) and vector (1 μg) for 24 h were infected with IAV (MOI = 0.2) for 2 h. The cellular IFN-α and IFN-β RNA levels were determined by qRT-PCR at 24 hpi. The experiments were performed in triplicate. Each value represents mean ± SD. $^{*}P < 0.05$; $^{**}P < 0.01$ versus Myc group.

the sensitivity of H1N1 and H3N2 viruses, which were consistent with the previous reports (Li *et al.* 2009; Iki *et al.* 2005). However, Li *et al.* showed that overexpression of PMLVI in MDCK cells conferred potent resistance to PR8 (H1N1) infection, while lacked inhibitory activity to ST1233 (H1N1), ST364 (H3N2), Qa199 (H9N2), and Ph2246 (H9N2) (Li *et al.* 2009). The different PML isoforms and different subtype influenza viruses may be responsible for the discrepancy.

Mechanistically, we found that PML inhibited the virus by regulating FBXW7-SHP2-RIG-I signaling pathway. It has been reported that the effect of FBXW7 on the innate immune response to inhibit virus relied on the interferon signaling pathway. Song *et al.* reported that FBXW7 translocated from nucleus into the cytoplasm during virus infection, which is critical for its antiviral function (Song *et al.* 2017). Despite PML proteins are primarily located in the nucleus, a small portion of PML is distributed in cytoplasm (Zhong *et al.* 1999). Therefore, we conducted Co-IP assay on the isolated cytoplasm and nuclear proteins respectively, and found that the interaction between PML and FBXW7 was both located in the cytoplasm and nuclear. The result suggested that PML may play an antiviral role through FBXW7 mediated downstream signaling pathway in cytoplasm. How does PML undergo nucleocytoplasmic shuttling? As we mentioned above, the localization of the majority of PML proteins was restricted to the nucleus due to the NLS locating in exon 6 of PML. However, a fraction of PML resides in the cytoplasm (Lin *et al.* 2004; Giorgi *et al.* 2010). In addition, PML provides sites for posttranslational modifications, for example, acetylation and phosphorylation sites surrounding the NLS (Hayakawa *et al.* 2008; Reineke *et al.* 2008) and it is reasonable to assume that these modifications by FBXW7 or other factors alter the accessibility to the NLS.

Increasing evidence suggests that E3 ligases play important roles in antiviral innate signaling. Although PML is a member of RBCC/TRIM family, the E3 ubiquitin ligase activity of PML has not been reported (Janer *et al.* 2006; Nisole *et al.* 2005). In this study, we demonstrated that PML maintained the stability of FBXW7 by inhibiting the K48-linked ubiquitination and degradation of FBXW7, which suggested that the interaction between PML and FBXW7 might inhibit the other E3 ubiquitin ligase to modify the FBXW7. However, this detail is not yet clear.

Previous study had showed that FBXW7 interacted with SHP2 and mediated the degradation and ubiquitination of SHP2 (Song *et al.* 2017), so we next studied the effect of PML on SHP2. The results showed that PML interacted with SHP2, and the interaction of PML with FBXW7 and SHP2, respectively, further enhanced the connection between FBXW7 and SHP2, and promoted the FBXW7-mediated degradation of SHP2. Three possible reasons may explain the results. First, the close binding between FBXW7 and SHP2 facilitated the recognition of SHP2 by FBXW7, which promoted ubiquitination and degradation. Second, PML increased the expression of FBXW7 and indirectly enhanced the E3 ubiquitin ligase activity of

FBXW7 and promoted the degradation of SHP2. Third, PML may degrade SHP2 through other ubiquitin–proteasome pathways, such as SUMO or NEDD, which need further study.

RIG-I recognized cytoplasmic influenza virus RNA, activated the downstream transcription factors IRF3 and IRF7, and induced type I interferon production, thus playing the role of antiviral natural immune regulator (Kell and Gale 2015). During RNA viral infection, SHP2 as a connector protein can connect the E3 ubiquitin ligase c-Cbl to the RIG-I to mediate k48-linked ubiquitination of RIG-I (Chen *et al.* 2013). Our results showed that the overexpression of PML inhibited RIG-I degradation by regulating SHP2, thus significantly increasing the mRNA level of *IFN-α* and *IFN-β*. Interestingly, the interferon can also induce the transcription and translation of PML and Sp100 in the PML-NBs, which further increased the number and volume of PML-NBs in the nucleus (Chelbi-Alix *et al.* 1995). Therefore, we believe that there is positive feedback regulation between PML and IFN.

In conclusion, PML upregulated the protein level of FBXW7 by inhibiting its K48-linked ubiquitination. Moreover, PML interacted with FBXW7 and SHP2 to form PML-FBXW7-SHP2 complexes, which promoted the degradation of SHP2. The reduction of SHP2 feedback maintained the stability of RIG-I and further promoted the production of type I interferon to inhibit the replication of the influenza virus. This research partly revealed the mechanism of PML on the influenza virus. The research on these host proteins not only helped to understand the replication of the influenza virus, but also provided a potential target for the development of novel treatment to combat influenza virus infection.

Acknowledgements The work was financially supported by National Science and Technology Major Projects for "Major New Drugs Innovation and Development" (2018ZX09711003), CAMS Initiative for Innovative Medicine (CAMS-I2M-1-010), and National Natural Science Foundation of China (81630089).

Author Contributions HYY, KL and YHL designed the experiments. HYY and MZ carried out the experiments. HYY, MZ and LY analyzed the data. HYY, HQW, and SW wrote the manuscript. KL and YHL finalized the manuscript. All authors read and approved the final manuscript.

Compliance with Ethical Standards

Conflict of interest No potential conflict of interest was reported by the authors.

Animal and Human Rights Statement This study does not contain any studies with human participants or animals performed by any of the authors.

References

Alandijany T, Roberts APE, Conn KL, Loney C, McFarlane S, Orr A, Boutell C (2018) Correction: distinct temporal roles for the promyelocytic leukaemia (PML) protein in the sequential regulation of intracellular host immunity to HSV-1 infection. PLoS Pathog 14:e1006927

Batty EC, Jensen K, Freemont PS (2012) PML nuclear bodies and other TRIM-defined subcellular compartments. Adv Exp Med Biol 770:39–58

Blondel D, Kheddache S, Lahaye X, Dianoux L, Chelbi-Alix MK (2010) Resistance to rabies virus infection conferred by the PMLIV isoform. J Virol 84:10719–10726

Chang HR, Munkhjargal A, Kim M-J, Park SY, Jung E, Ryu J-H, Yang Y, Lim J-S, Kim Y (2018) The functional roles of PML nuclear bodies in genome maintenance. Mutat Res/fundam Mol Mech Mutagen 809:99–107

Chelbi-Alix MK, Pelicano L, Quignon F, Koken MH, Venturini L, Stadler M, Pavlovic J, Degos L, de Thé H (1995) Induction of the PML protein by interferons in normal and APL cells. Leukemia 9:2027–2033

Chelbi-Alix MK, Quignon F, Pelicano L, Koken MH, de Thé H (1998) Resistance to virus infection conferred by the interferon-induced promyelocytic leukemia protein. J Virol 72:1043–1051

Chelbi-Alix MK, Vidy A, El Bougrini J, Blondel D (2006) Rabies viral mechanisms to escape the IFN system: the viral protein P interferes with IRF-3, Stat1, and PML nuclear bodies. J Interferon Cytokine Res 26:271–280

Chen W, Han C, Xie B, Hu X, Yu Q, Shi L, Wang Q, Li D, Wang J, Zheng P, Liu Y, Cao X (2013) Induction of Siglec-G by RNA viruses inhibits the innate immune response by promoting RIG-I degradation. Cell 152:467–478

Chen D, Feng C, Tian X, Zheng N, Wu Z (2018) Promyelocytic leukemia restricts enterovirus 71 replication by inhibiting autophagy. Front Immunol 9:1268

El Asmi F, Maroui MA, Dutrieux J, Blondel D, Nisole S, Chelbi-Alix MK (2014) Implication of PMLIV in both intrinsic and innate immunity. PLoS Pathog 10:e1003975

Everett RD, Chelbi-Alix MK (2007) PML and PML nuclear bodies: implications in antiviral defence. Biochimie 89:819–830

Giorgi C, Ito K, Lin HK, Santangelo C, Wieckowski MR, Lebiedzinska M, Bononi A, Bonora M, Duszynski J, Bernardi R, Rizzuto R, Tacchetti C, Pinton P, Pandolfi PP (2010) PML regulates apoptosis at endoplasmic reticulum by modulating calcium release. Science 330:1247–1251

Hayakawa F, Abe A, Kitabayashi I, Pandolfi PP, Naoe T (2008) Acetylation of PML is involved in histone deacetylase inhibitor-mediated apoptosis. J Biol Chem 283:24420–24425

Hsu KS, Kao HY (2018) PML: regulation and multifaceted function beyond tumor suppression. Cell Biosci 8:5

Iki S, Yokota S, Okabayashi T, Yokosawa N, Nagata K, Fujii N (2005) Serum-dependent expression of promyelocytic leukemia protein suppresses propagation of influenza virus. Virology 343:106–115

Inuzuka H, Shaik S, Onoyama I, Gao D, Tseng A, Maser RS, Zhai B, Wan L, Gutierrez A, Lau AW, Xiao Y, Christie AL, Aster J, Settleman J, Gygi SP, Kung AL, Look T, Nakayama KI, DePinho RA, Wei W (2011) SCFFBW7 regulates cellular apoptosis by targeting MCL1 for ubiquitylation and destruction. Nature 471:104–109

Janer A, Martin E, Muriel MP, Latouche M, Fujigasaki H, Ruberg M, Brice A, Trottier Y, Sittler A (2006) PML clastosomes prevent nuclear accumulation of mutant ataxin-7 and other polyglutamine proteins. J Cell Biol 174:65–76

Kell AM, Gale M Jr (2015) RIG-I in RNA virus recognition. Virology 479–480:110–121

Kentsis A, Dwyer EC, Perez JM, Sharma M, Chen A, Pan ZQ, Borden KL (2001) The RING domains of the promyelocytic leukemia protein PML and the arenaviral protein Z repress translation by directly inhibiting translation initiation factor eIF4E. J Mol Biol 312:609–623

Krammer F, Palese P (2015) Advances in the development of influenza virus vaccines. Nat Rev Drug Discov 14:167–182

Li W, Wang G, Zhang H, Zhang D, Zeng J, Chen X, Xu Y, Li K (2009) Differential suppressive effect of promyelocytic leukemia protein on the replication of different subtypes/strains of influenza A virus. Biochem Biophys Res Commun 389:84–89

Li K, Wang F, Cao WB, Lv XX, Hua F, Cui B, Yu JJ, Zhang XW, Shang S, Liu SS, Yu JM, Han MZ, Huang B, Zhang TT, Li X, Jiang JD, Hu ZW (2017) TRIB3 promotes APL progression through stabilization of the oncoprotein PML-RARα and inhibition of p53-mediated senescence. Cancer Cell 31:697-710.e697

Lin HK, Bergmann S, Pandolfi PP (2004) Cytoplasmic PML function in TGF-beta signalling. Nature 431:205–211

Maul GG, Guldner HH, Spivack JG (1993) Modification of discrete nuclear domains induced by herpes simplex virus type 1 immediate early gene 1 product (ICP0). J Gen Virol 74:2679–2690

Moberg KH, Bell DW, Wahrer DC, Haber DA, Hariharan IK (2001) Archipelago regulates Cyclin E levels in Drosophila and is mutated in human cancer cell lines. Nature 413:311–316

Negorev D, Maul GG (2001) Cellular proteins localized at and interacting within ND10/PML nuclear bodies/PODs suggest functions of a nuclear depot. Oncogene 20:7234–7242

Nisole S, Stoye JP, Saïb A (2005) TRIM family proteins: retroviral restriction and antiviral defence. Nat Rev Microbiol 3:799–808

Nisole S, Maroui MA, Mascle XH, Aubry M, Chelbi-Alix MK (2013) Differential roles of PML isoforms. Front Oncol 3:125

Reineke EL, Lam M, Liu Q, Liu Y, Stanya KJ, Chang KS, Means AR, Kao HY (2008) Degradation of the tumor suppressor PML by Pin1 contributes to the cancer phenotype of breast cancer MDA-MB-231 cells. Mol Cell Biol 28:997–1006

Scherer M, Stamminger T (2016) Emerging role of PML nuclear bodies in innate immune signaling. J Virol 90:5850–5854

Shaw ML, Stertz S (2018) Role of host genes in influenza virus replication. Curr Top Microbiol Immunol 419:151–189

Song Y, Lai L, Chong Z, He J, Zhang Y, Xue Y, Xie Y, Chen S, Dong P, Chen L, Chen Z, Dai F, Wan X, Xiao P, Cao X, Liu Y, Wang Q (2017) E3 ligase FBXW7 is critical for RIG-I stabilization during antiviral responses. Nat Commun 8:14654

Tsunematsu R, Nakayama K, Oike Y, Nishiyama M, Ishida N, Hatakeyama S, Bessho Y, Kageyama R, Suda T, Nakayama KI (2004) Mouse Fbw7/Sel-10/Cdc4 is required for notch degradation during vascular development. J Biol Chem 279:9417–9423

Wang R, Wang Y, Liu N, Ren C, Jiang C, Zhang K, Yu S, Chen Y, Tang H, Deng Q, Fu C, Wang Y, Li R, Liu M, Pan W, Wang P (2013) FBW7 regulates endothelial functions by targeting KLF2 for ubiquitination and degradation. Cell Res 23:803–819

Wang G, Tian Y, Hu Q, Xiao X, Chen S (2018) PML/RARa blocks the differentiation and promotes the proliferation of acute promyelocytic leukemia through activating MYB expression by transcriptional and epigenetic regulation mechanisms. J Cell Biochem. https://doi.org/10.1002/jcb.27077

Welcker M, Clurman BE (2008) FBW7 ubiquitin ligase: a tumour suppressor at the crossroads of cell division, growth and differentiation. Nat Rev Cancer 8:83–93

Yada M, Hatakeyama S, Kamura T, Nishiyama M, Tsunematsu R, Imaki H, Ishida N, Okumura F, Nakayama K, Nakayama KI (2004) Phosphorylation-dependent degradation of c-Myc is mediated by the F-box protein Fbw7. Embo J 23:2116–2125

Zhong S, Hu P, Ye TZ, Stan R, Ellis NA, Pandolfi PP (1999) A role for PML and the nuclear body in genomic stability. Oncogene 18:7941–7947